ELSEVIER

thin solid films

Thin Solid Films 335 (1998) 117-121

Effect of substrate heating on elimination of pinholes in sputtering deposited SiO_2 films on $LiNbO_3$ single crystal substrates

Hirotoshi Nagata[a,*], Tetsuya Fujino[b], Naoki Mitsugi[a], Masumi Tamai[c]

[a] *Optoelectronics Research Division of New Technology Research laboratories, Sumitomo Osaka Cement Co., Ltd., 585 Toyotomi-cho, Funabashi-shi, Chiba 274-8601, Japan*

[b] *Optoelectronics & Electronics Division, Sumitomo Osaka Cement Co., Ltd., 585 Toyotomi-cho, Funabashi-shi, Chiba 274-8601, Japa*

[c] *Advanced Materials Research Division of New Technology Research Laboratories, Sumitomo Osaka Cement Co., Ltd., 585 Toyotomi-cho, Funabashi-shi, Chiba 274-8601, Japan*

Received 4 March 1998; accepted 12 June 1998

Abstract

In the fabrication of high-speed Ti:$LiNbO_3$ optical waveguide modulators, the sputtering deposition of 1μ m-thick-order SiO_2 films on $LiNbO_3$ substrates and the subsequent O_2 atmosphere annealing are key processes. However, large numbers of pinholes appear in the films after the annealing process limiting the fabrication yield. Here, we demonstrate that such pinholes are eliminated in films deposited on heated $LiNbO_3$ substrates. In addition to the common effect of increased film adhesive strength and density, the reduction in H_2O impurities in $LiNbO_3$ and SiO_2 by substrate heating is considered to be the reason for this phenomenon. © 1998 Elsevier Science S.A. All rights reserved.

Keywords: Oxides; Optoelectronic devices; Sputtering deposition; SiO_2; $LiNbO_3$

1. Introduction

Recent research on oxide materials is mainly focused on the synthesis of exotic, function-harmonized materials, such as perovskite based ferroelectric, ferromagnetic, and superconducting crystals [1-3]. However, in order to apply these attractive oxides to practical devices, we must first conduct an investigation into device fabrication technology. Actually, various kinds of oxide-based devices have been made. But the fabrication processes for these devices are used without regard to certain problems caused by oxide crystals [4,5].

$LiNbO_3$ is one of such promising materials, especially for integrated optical waveguide components. In fact, $LiNbO_3$-based optical modulators have already been installed in world-wide optical fiber communication systems [6]. However, while present $LiNbO_3$ modulator devices are produced via conventional photolithography, thin film deposition and dry etching technologies, many technical problems characteristic to the $LiNbO_3$ process, have been found. For instance, during the fluorocarbon plasma etching of a $LiNbO_3$ surface, LiF-based particles were found to precipitate and cause mechanical failure in the devices as previously reported by Nagata et al. [7,8]. In this paper, the Problem appearing during the SiO_2 film formation process is analyzed, because the SiO_2 buffer layer is an important element in the development of high-speed $LiNbO_3$ optical modulators. The main problem of focus was the generation of pinholes in films after high temperature annealing which followed the sputtering process.

2. pinhole generation in SiO_2 films on $LiNbO_3$

On $LiNbO_3$ single crystal wafers, which include optical waveguides formed by thermal diffusion of Ti, SiO_2 buffer layers are deposited by either a vacuum evaporation method or an rf-magnetron sputtering method. However, with the increasing demand for high-speed operation at over 20Gb/s, a dense SiO_2 buffer layer deposited via the sputtering method is preferable because it can achieve a highly effective electro-optic interaction between the electrodes and the waveguides. Furthermore, a film thickness of over 1É m is needed to obtain a suitable electrical impedance matching, etc. between the Au electrodes and the $LiNbO_3$ substrate.

We found that during such dense and thick SiO_2 film deposition on $LiNbO_3$ substrates, the inevitably high internal film stress induced mechanical failures . such as large substrate deflections and broken substrates. In addition to

*Corresponding author. Fax: +81 474 57 3993;
e-mail: LDT00246@niftyserve.or.jp.

0040-6090/98/$ - see front matter C 1998 Elsevier Science S.A. All rights reserved.
Pll S0040-6090(98)00967-5

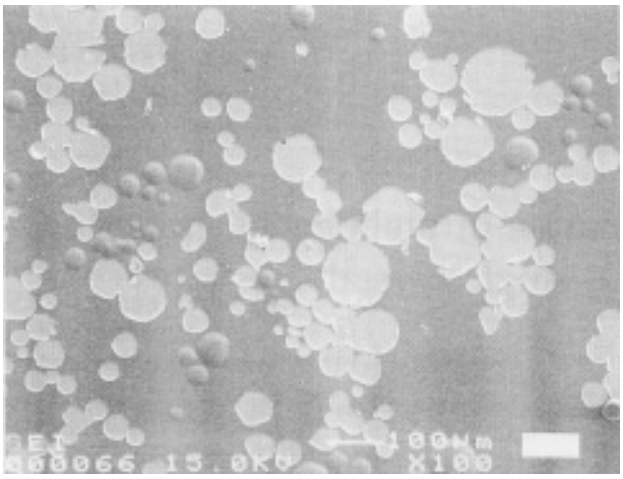

Fig. 1. SEM image of pinholes appeared in a 0.7 μm thick SiO_2 film on a $LiNbO_3$ wafer after post-annealing at 600ºC for 5h in flowing O_2. The bar in the figure denotes 100 μm length.

such general phenomena independent of the substrates, many pinholes were frequently observed in sputtering deposited SiO_2 films on $LiNbO_3$ after post-annealing. Furthermore, there was a tendency in the number of pinholes to increase significantly for thicker films (approx. 1 μm). In the actual device fabrication process, the deposition and post-annealing of thinner films has to be repeated a few times to suppress the development of pinholes. However, in order to improve the device fabrication yield, we explored possible reasons for the generation of pinholes and developed a method to completely eradicate them.

Fig. 1 shows a secondary electron microscopic (SEM) image of the typical pinholes that appeared in a 0.7 μm-thick SiO_2 film on a 3 inch diameter z-cut $LiNbO_3$ wafer after post-annealing at 600ºC for 5 h in flowing O_2. Circular pinholes with l0-100 μm diameters were observed throughout the annealed wafer surface, while no pinhole was observed before annealing. The step height of the pinholes, measured by a stylus method, was the same as the thickness of the deposited film. Furthermore, an Auger electron spectroscopy (AES) was carried out on the bottom surface of the pinholes and no specific contaminant element was detected except for Nb from the $LiNbO_3$ and C with the same amount of that from the SiO_2 surface. These results, at the very least, indicate that the SiO_2 film was removed from the $LiNbO_3$ surface by the annealing and generated many pinholes.

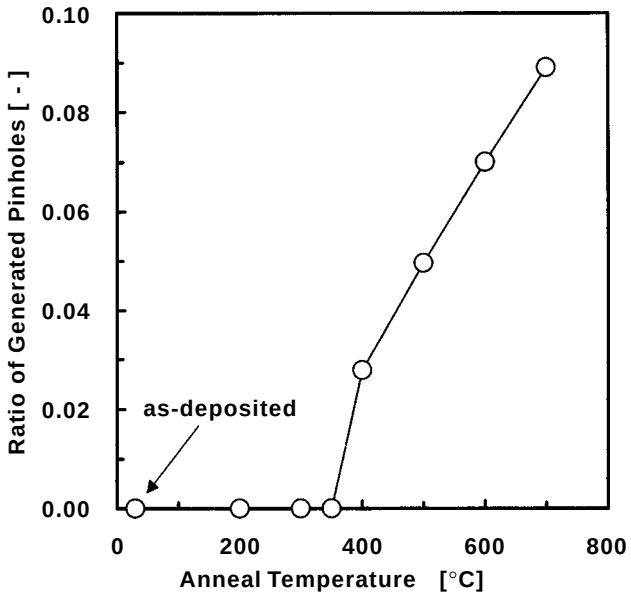

Fig. 2. The presence of pinholes, denoted by a ratio of the total width of pinholes measured to the total length of the surface measured, relative to annealing temperature.

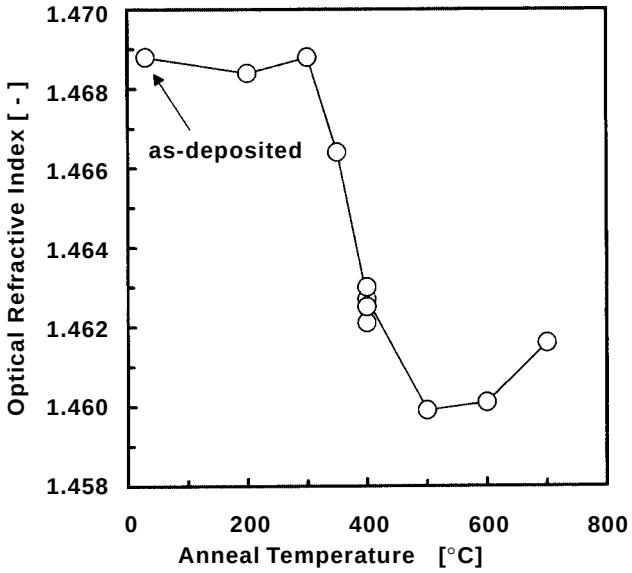

Fig. 3. The optical refractive index of the SiO_2 films measured at wavelength of 633 nm relative to annealing temperature.

In order to understand what influence the post-annealing temperature has on pinhole generation, a 1.2 μm thick SiO_2 film was deposited on a $LiNbO_3$ wafer and cut into 10 × 10 mm pieces, and then annealed under various heating conditions. The film was prepared by conventional rf-magnetron sputtering using the SiO_2 target and Ar/O_2 (=5/1 and approx. 0.4 Pa) mixture without intentional substrate heating. The deposition rate was 0.17-0.18nm/s. The deposited film was smooth without any pinholes even after the wafer cutting process. Before and after annealing, the surface morphology and optical refractive index of the film were examined.

Fig. 2 shows a change in the prevalence of pinholes, depending on the annealing temperature, As an index for the amount of pinholes, a 5×5 mm area of the samples was scanned by a stylus profilometer with a 0.5-mm interval between each scan, and the ratio of the total length of the pinhole bottoms ($LiNbO_3$ surface) measured to the total scan length (sum of lengths for the remaining film surface and the pinhole bottom) was calculated and plotted on the vertical axis of Fig. 2. In the experiments, the heating rate to

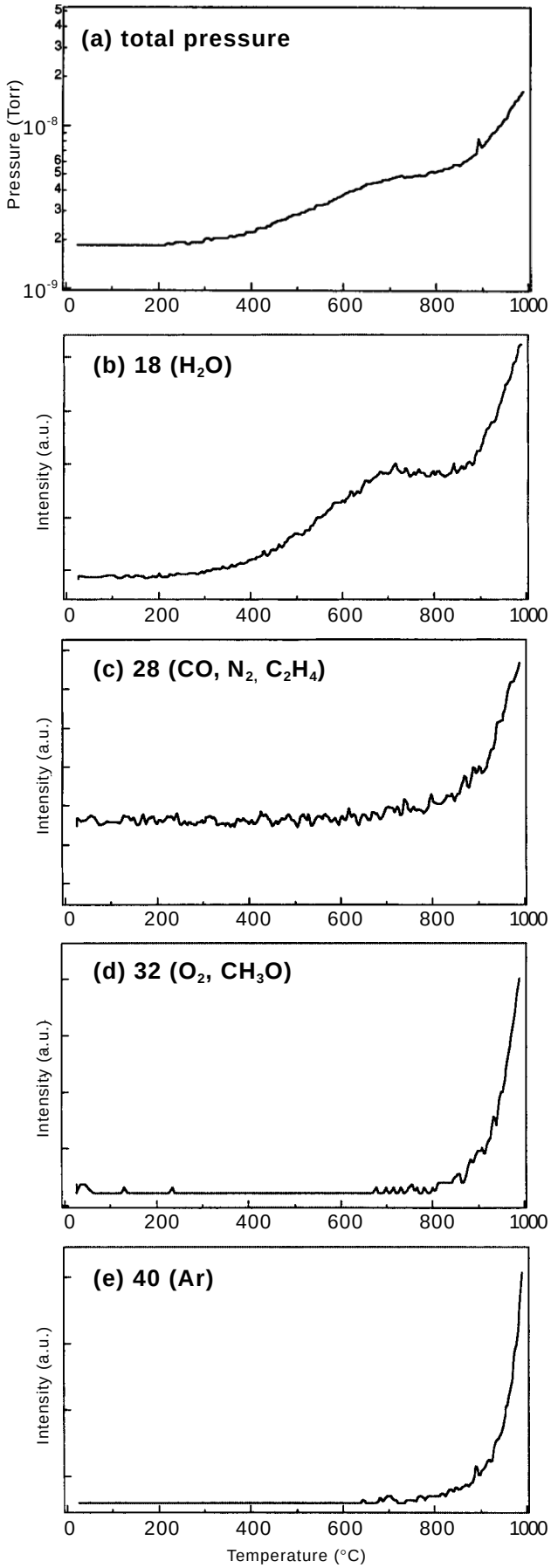

Fig. 4. TDS profiles of SiO_2 films on $LiNbO_3$ for (a) change of the total pressure due to thermal decomposition of the sample, (b) evaporation of fragment 18 (H_2O), (c) fragment 28 (possibly due to organic contaminants), (d) fragment 32 (possibly due to O_2 and organic contaminants) and (e) fragment 40 (Ar).

a certain annealing temperature and the holding time were fixed at 5 K/min and 5 h, respectively, while O_2 Was introduced into the furnace at a rate of 500cm^3/min. The cooling was done by simply turning off the heater. As shown, the generation of pinholes occurred at annealing temperatures beyond 350ºC and became more frequent with increased temperature. With respect to annealing at 400ºC, in order to determine the effect of heating rate, we attempted to heat at both a slower rate of 1 K/min and at a sudden shift to 400ºC after 5 h of annealing at 300ºC These methods produced similar results. We thus concluded that the generation of pinholes was mainly affected by the annealing temperature itself.

Annealing below 350ºC was the most effective method to prevent (mitigate) the formation of pinholes, but annealing at 600ºC was necessary to obtain a steadily oxidized SiO_2 buffer layer. Fig. 3 reveals the change in the optical refractive index of the SiO_2 films depending on the annealing temperature. The refractive index was measured using a prism-coupler at an optical wavelength of 633nm. The refractive index of the as-deposited SiO_2 films decreased by oxygen atmosphere annealing mainly due to the increase in the level of oxygen in the film. For the present films, as shown in Fig. 3, the refractive index decreased at temperatures beyond 350ºC and reached a minimum at temperatures between 500 and 600ºC. At 700ºC, the refractive index increased again, possibly due to a chemical interaction between $LiNbO_3$ and SiO_2, such as a diffusion of Li. The results supported the theory that O_2 annealing at 500-600ºC was the process necessary to obtain steadily oxidized SiO_2 films, although such high temperature annealing caused the formation of pinholes in films.

3. Elimination of pinholes by substrate heating

Thermal decomposition and evaporation of the contamination in the constituent materials was considered to be the reason for the generation of pinholes. In Fig. 1, few hill-like defects having sizes corresponding to pinholes, were observed, and they were considered to be caused by a generation of gases at the film/substrate boundary. The decomposition of organic contamination existing on the $LiNbO_3$ surface and the evaporation of molecular contamination in the $LiNbO_3$ were assumed to be possible origins of the gases.

At first, the effect of cleaning the surface of the $LiNbO_3$ wafer before the SiO_2 film deposition process was investigated. Some wet cleaning methods were used, but no difference was observed in the pinhole generation behavior.

These methods included ultrasonic cleaning in a commercial detergent or an acetone/ethyl alcohol mixture, and the amount of organic contamination was measured to decrease to 30-60 pg/cm^2 (mainly benzene and phthalic acid) from 4000 pg/cm^2 before cleaning. Here, the level of contamination was measured by gas chromatography accompanied with mass spectroscopy (GC/MS) of the thermally decomposed fragments of the surface contamination at 400ºC. On the other hand, a dry etching cleaning of the surface by oxygen plasma was also attempted just before the film deposition in the same process chamber. This method, too, caused no notable reduction in the number of pinholes.

Then, in order to check the contaminant fragments actually evaporating from the SiO_2 films on the $LiNbO_3$, a thermal decomposition spectroscopy (TDS) analysis was carried out for the 1.2 μm-thick SiO_2 films prepared similarly to the samples shown in Figs. 2 and 3. Films were deposited on both sides of the $LiNbO_3$ to exclude the fragments directly evaporated from the $LiNbO_3$ from our measurements. In the measurements, a 6 × 6 mm square sample was heated in a vacuum (6×10^{-7} Pa) up to 1000ºC at 60 K/min, while windows of the mass detector were set at 17, 18, 20, 28, 32, and 40. Fragments having mass number 17 and 18 were considered to come mainly from H_2O, fragments 20 and 40 were from Ar, fragment 28 was from CO, N_2, C_2H_4, etc. and fragment 32 was from O_2, CH_3O, etc. Fig. 4 shows the TDS profiles for (a) a change of the total pressure due to thermal decomposition of the sample, (b) evaporation of the fragment 18 (H_2O), (c) fragment 28 (possibly due to organic contaminants), (d) the fragment 32 (possibly due to O_2 and organic contaminants), and (e) the fragment 40 (Ar). As can be seen, the dominant fragment evaporated from the SiO_2 on $LiNbO_3$ was identified as H_2O (see Fig. 4b), and no fragment due possibly to organic contamination was found below 800ºC. Furthermore, the evaporation of H_2O began at about 300ºC and saturated at 700-800ºC. This behavior seemed to correspond with changes in the amount of pinholes (Fig. 2) and the refractive index (Fig. 3). Therefore, we considered that the thermal decomposition and the evaporation of H_2O impurities in the materials were plausible origins of pinholes.

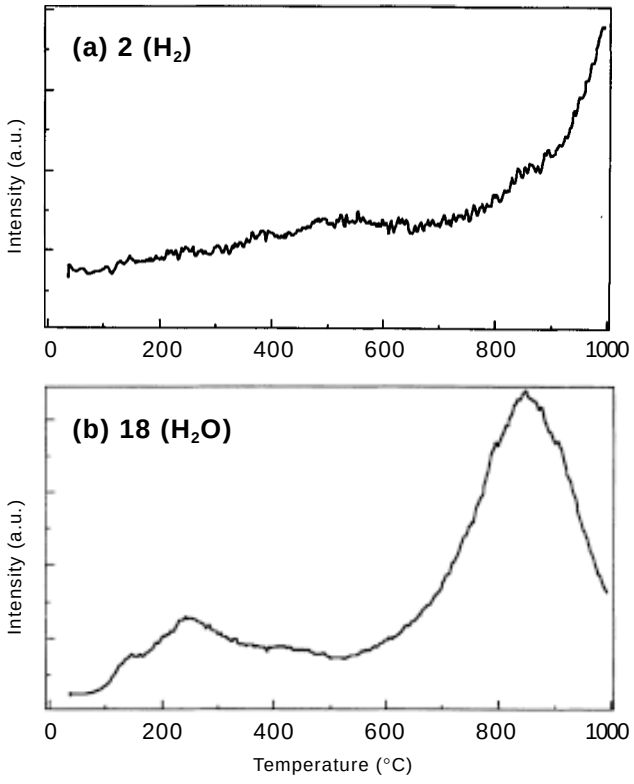

Fig. 5. TDS profiles of the $LiNbO_3$ substrate for (a) fragment 2 (H_2) and (b) fragment 18 (H_2O).

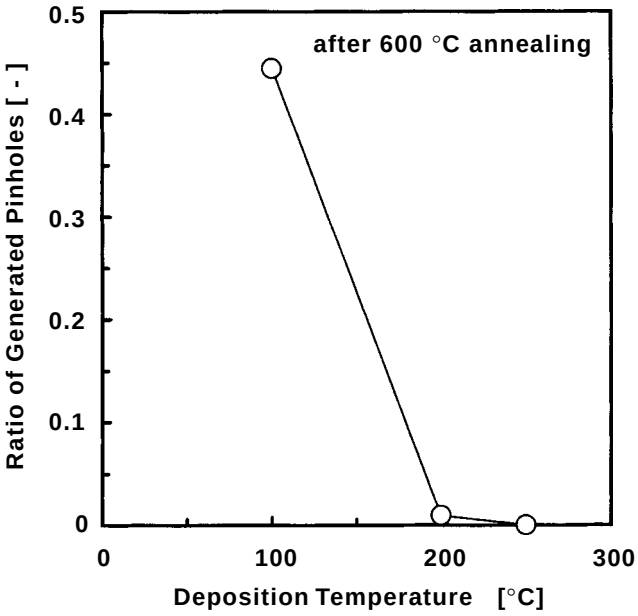

Fig. 6. The relationship between substrate temperatures during the approx. 1 μm thick film depositions and the amount of pinholes after post-annealing at 600ºC for 5 h. The presence of pinholes, denoted by a ratio of the total width of pinholes measured to the total length of the surface measured, relative to annealing temperature.

In order to track the possible origin of the H_2O, a z-cut $LiNbO_3$ sample was similarly investigated by TDS. Fig. 5 shows the TDS profiles for fragments 2 (H_2) and 18 (H_2O), respectively. The $LiNbO_3$ crystal could have H_2O impurities as the H on Li sites and as the OH in O-O planes normal to the z-axis. The results suggest that the $LiNbO_3$ wafer itself could become the source of H_2O at elevated temperatures.

From the above experimental results, we surmised that substrate heating during the SiO_2 deposition could be effective in reducing H_2O impurities both in the $LiNbO_3$ substrates and the growing films. Fig. 6 shows the relationship between substrate temperatures during approx. 1É m thick film depositions and amounts of pinholes that appear after post-annealing at 600ºC for 5 h. By the 200ºC deposition, the generation of pinholes could be significantly reduced and almost completely eliminated by the 250ºC

deposition. Considering the results of Fig. 5, the H_2O impurity in the $LiNbO_3$ could be partially removed by heating at 200-250ºC beforehand to prevent (mitigate) H_2O evaporation at the film/$LiNbO_3$ boundary during post-annealing.

Similar depositions at 250ºC and post-annealing was carried out more than five times using 3-inch diameter $LiNbO_3$ wafers, and no pinholes have been detected yet by optical microscopic observation. The refractive indices at 633nm wavelength for these SiO_2 films were measured to be 1.468 before post-annealing and 1.462 after annealing. On the other hand, the film deposited without substrate heating showed a refractive index of 1.460 after annealing (see Fig. 3), suggesting that the film density was also improved by substrate heating.

4. Conclusion

The generation of pinholes in sputtering deposited SiO_2 films on $LiNbO_3$ after post-annealing at 400-700ºC could be successfully suppressed by carrying out the deposition at elevated temperatures, preferably beyond 250ºC. The results can be effectively applied to the fabrication of high-speed Ti:$LiNbO_3$ optical waveguide modulators, especially those over 20 Gb/s, because the sputtering deposition of 1-1.5 μm SiO_2 films on $LiNbO_3$ substrates and the O_2 atmosphere annealing that follows are key processes to satisfy the design demand on constituent materials for these devices. From our impurity analysis results, we concluded that the reason for the elimination of pinholes was reduction of H_2O impurities in $LiNbO_3$ and SiO_2 by substrate heating, in addition to common effect of increased film adhesive strength and density.

Acknowledgements

This study was supported by Special Coordination Funds for Promoting Science and Technology 'Fundamental research on new materials of function-harmonized oxides,' from the Japanese Science and Technology Agency.

Ref erences

[1] H. Koinuma, MRS Bulletin 19 (1994) 21.
[2] O. Auciello, R. Ramesh, MRS Bulletin 21 (1996) 21.
[3] O. Auciello, R. Ramesh, MRS Bulletin 21 (1996) 29.
[4] H. Nagata, J. Ichikawa, Opt. Eng. 34 (1995) 3284.
[5] M.A. Powell, A.O. Donnell, Opt. Phot. News, 8, September (1997) 23.
[6] R.C. Alferness, Opt. Phot. News, 8, September (1997) 16.
[7] K. Shima, N. Mitsugi, H.J. Nagata, Mater. Res. 13 (1998) 527.
[8] H. Nagata, N. Mitsugi, K. Shima, M. Yamai, E.M. Haga, J. Cryst. Growth 187 (1998) 573.